Half-life measurements of proton-rich ^{78}Kr fragments

M. J. López Jiménez,[1] B. Blank,[1] M. Chartier,[1] S. Czajkowski,[1] P. Dessagne,[2] G. de France,[3] J. Giovinazzo,[1] D. Karamanis,[1] M. Lewitowicz,[3] V. Maslov,[4] C. Miehé,[2] P. H. Regan,[5] M. Stanoiu,[3] and M. Wiescher[6]

[1]*Centre d'Etudes Nucléaires de Bordeaux-Gradignan, Le Haut-Vigneau, Boîte Postale 120, F-33175 Gradignan, France*

[2]*Institut de Recherches Subatomiques, 22 rue du Loess, Boîte Postale 28, F-67037 Strasbourg Cedex 2, France*

[3]*Grand Accélérateur National d'Ions Lourds, Boîte Postale 5027, F-14076 Caen Cedex, France*

[4]*Flerov Laboratory of Nuclear Reactions, Joint Institute for Nuclear Research, 141980 Dubna, Russia*

[5]*Department of Physics, University of Surrey, Guildford, Surrey GU2 7XH, United Kingdom*

[6]*Department of Physics, University of Notre Dame, Notre Dame, Indiana 46556*

(Received 12 April 2002; published 27 August 2002)

The β^+ decay half-lives of 22 neutron-deficient nuclei in the cobalt-to-krypton region have been measured following the fragmentation of a primary ^{78}Kr beam at an energy of 73 MeV per nucleon. The half-lives of the $T_z=-1$ nuclei ^{62}Ge, ^{64}As, and ^{66}Se are determined for the first time with values of (129 ± 35) ms, 18^{+43}_{-7} ms, and (33 ± 12) ms, respectively. The impact of these results on the nucleosynthesis and time scale of the astrophysical rapid proton-capture process are discussed.

DOI: 10.1103/PhysRevC.66.025803 PACS number(s): 23.40.−s, 21.10.−k

I. INTRODUCTION

Nuclei close to the proton drip line with $Z=30-40$ are of particular interest for the simulation of the thermonuclear runaway on the surface of accreting neutron stars, observed as *x*-ray bursts [1]. The runaway is driven by the rapid proton-capture process (RP process) which is described as a sequence of proton-capture reactions and β decays along the proton drip line [2]. The runaway is halted by the ^{56}Ni(p,γ)-^{57}Cu(γ,p) equilibrium at peak temperatures in excess of 2 GK [3]. During the subsequent cooling phase the RP process reignites and the reaction path is determined by the competition of proton-capture reactions and β^+ decays along the $N=Z$ line up to an endpoint region in the Sn-Te mass range [4]. It has been shown that such an RP process could produce the progenitor isotopes of the light *p* nuclei (^{92,94}Mo,^{96,98}Ru) whose nucleosynthesis site of origin is still a matter of debate [5]. Such a scenario requires that a fraction of less than 1% of the processed material escapes the gravitational potential of the accreting neutron star.

The detailed reaction path of the RP process depends on the masses of the associated nuclei [3]. At the high temperature conditions of an x-ray burst, proton capture is typically considerably faster than the competing β decay; at the drip line, further processing depends on the β-decay lifetime of the drip-line nuclei as compared to the cooling time of the x-ray burst environment. Therefore β-decay lifetime studies are an important ingredient for determining the time scale for rapid nucleosynthesis processes. The RP process has reached a waiting point if the cooling rate is distinctively faster than the decay rate, the temperatures will be too low and further proton-capture reactions are inhibited by the large Coulomb barrier. If the cooling is slow, the process continues beyond the waiting point until it reaches eventually the endpoint region of the rp-process where the remaining hydrogen fuel is burned by the Sn-Te cycle [4].

Of particular relevance are the $N=Z$ waiting points ^{60}Zn, ^{64}Ge, ^{68}Se, and ^{72}Kr because of their relatively long lifetimes [6]. The observation of ^{60}Ga [7] and ^{65}As is also of particular interest as these proton drip line, odd-Z nuclei might open up new capture branches for the RP process to synthesize heavier nuclei. On the other hand, the fact that ^{69}Br [7] is unbound might significantly hinder the RP process to produce heavier nuclei due to the rather long half-life (35.5 s) of ^{68}Se.

A particular case is the competition between β decay and the two-proton capture. The production of nuclei heavier than $A=68$ in x-ray bursts can be strongly enhanced by the two-proton capture reaction on ^{68}Se [3]. In this reaction sequence, proton scattering on ^{68}Se produces a small equilibrium abundance of proton-unbound ^{69}Br nuclei [7], which then capture another proton producing ^{70}Kr. The β decay out of the $N=34$ isotone chain then occurs at ^{70}Kr [8].

In the present paper, we report on half-life measurements for proton-rich nuclei between $Z=27$ and $Z=36$ which are important in modeling the RP process through the thermonuclear runaway after reignition through the ^{56}Ni(p,γ) reaction.

II. EXPERIMENTAL METHOD

The experiment was performed by means of the LISE spectrometer [9] at GANIL. We used the fragmentation of a primary 73 MeV/nucleon ^{78}Kr^{34+} beam with an average intensity of 2 μA. Three different settings were used. In two settings, the secondary beam was produced in the SISSI-ALPHA spectrometer [10] with a 177.8 mg/cm^2 thick carbon target combined with a thin degrader (50 μm of beryllium) at the LISE dispersive focal plane. In one of these two settings, the optimized fragment was the unbound ^{64}Se nucleus, while in the second case the optimized fragment was ^{69}Kr. Finally in the third setting, the secondary beam was produced at the LISE target position with a 1031 μm thick beryllium target and the same degrader with the beam line optimized for ^{69}Kr.

At the final focus, the fragments were stopped in a four-element silicon telescope (see Fig. 1). The first element consisted of a 500 μm thick energy loss (ΔE) detector. A

 ©2002 The American Physical Society

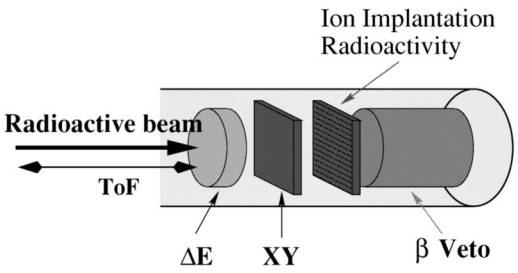

FIG. 1. The detection setup used in the present experiment consisted of a four-element silicon-detector telescope with a double-sided silicon strip detector of 300 μm as the implantation device.

500 μm thick position-sensitive detector was placed behind the ΔE detector. A double-sided silicon strip detector (16 $\times$16 strips) was used as the implantation device (300 μm). Finally, at the back of the telescope, a fourth Si(Li) detector, of thickness 6 mm, was used to discriminate against any contaminant lighter ions which reached the final focus. A time of flight (TOF) for the fragments from the production target to the silicon telescope was determined by measuring the time difference between a fast signal extracted from the ΔE detector and the cyclotron radiofrequency. This TOF, together with the energy loss in the ΔE detector and the magnetic rigidity of the dipole magnets in the LISE3 spectrometer was used to obtain an unambigous identification in Z and N for each fragment (see Fig. 2), using previously described techniques [7,11].

III. DATA ANALYSIS AND RESULTS

The β^+ decay half-lives of fragments were not determined by the classical method, i.e., by switching off the beam after implantation of a fragment by a hardware trigger [12], but we rather used a continous beam and determined the half-lives in the following way. In the off-line analysis, cuts were applied to a two-dimensional particle identification matrix of ΔE versus TOF. After an implantation, subsequent

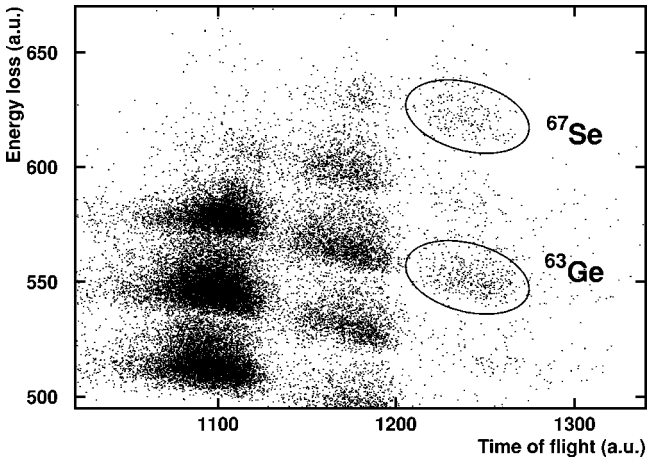

FIG. 2. Two-dimensional identification plot of energy loss in the first silicon detector vs the TOF between the production target and the silicon detector. This plot corresponds to the setting on ^{69}Kr using the LISE target.

β^+ decays were correlated with all previous implants in the same pixel of the silicon strip detector during a 5 s period. To obtain a β^+-decay time spectrum, the time difference between the ion implantation and any subsequent decay signal in the same pixel was determined. Uncorrelated radioactivity events contributed to a constant background level in the time spectra. The high background level in the decay-time spectra comes from the fact that any decay event is correlated to any implantation occuring prior to the decay event. Thus, a lot of ''wrong'' correlations generate a constant background.

The half-lives of the radioactive decays were obtained by applying a fit to the data with a function composed of an exponential decay plus a constant background level. For nuclei with short-lived daughters, the daughter decay was taken into account (see below).

As can be seen from Fig. 2, the separation between neighboring nuclei, especially for the energy loss, is not perfect. To get clean decay spectra in cases where neighboring nuclei have similar half-lives, only implantation events from the interior part of the ΔE-TOF zone for a given nuclide were used to generate the half-life spectra.

The present experiment allowed half-life measurements of 22 different nuclear species. These data are summarized in Table I. They are compared with previously published experimental values and mean values have been calculated. All fits have been done using a correlation interval of 5 s. In the following sections where we discuss the results of different groups of nuclei, shorter time intervals were used for presenting the results. Half-life values obtained in this work are indicated in the figures.

A. $T_z=0$: ^{54}Co, ^{56}Ni, ^{58}Cu, ^{60}Zn, ^{62}Ga, ^{64}Ge, ^{66}As, ^{68}Se, and ^{70}Br

Half-lives of odd-odd, $N=Z$ nuclei were used to determine the universal ft value for Fermi superallowed transitions [35]. After small corrections, the involved $0^+\rightarrow 0^+$ transitions can be used to test the standard model of the weak interaction via the conserved vector current (CVC) hypothesis. Ingredients for these tests are precise Q_β values as well as high-precision partial decay half-lives. Although the high precision needed for these tests (10^{-4}) has not yet been reached for all of these nuclei, the half-lives of ^{54}Co, ^{58}Cu, ^{62}Ga, ^{66}As, and ^{70}Br are known with a good precision (better than 10^{-2} except for ^{58}Cu which due to its $T=0$, $I^\pi=1^+$ ground state has a longer half-life than the others).

In the experiment we present here, the decay of these nuclei (see Fig. 3) was used as a reference to test the analysis procedure of the current work. Our results for the odd-odd, $N=Z$ nuclei agree for all cases with the literature values (see Table I). However, only the nuclei ^{62}Ga and ^{66}As are produced with reasonable statistics to allow for a high-precision comparison. Our analysis yields half-lives of (114 ± 2) ms and (97 ± 2) ms for ^{62}Ga and ^{66}As, respectively, which may be compared to the literature values of (116.12 ± 0.22) ms [15–17] and (95.77 ± 0.22) ms [16,18]. For ^{54}Co, ^{58}Cu, and ^{70}Br, the production rate was too low to allow for a more detailed comparison. For the lower-Z nuclei, the background increases, as the identification is more and more polluted by

TABLE I. Summary of half-life values for isotopes with $T_z \leq 0$ between $Z=27$ and $Z=36$. Values obtained in the present work are compared to results of previous work. The mean value is an error-weighted average of the experimental data. For mean values with an asterisk, see the discussion in the text. The last column gives the half-life values used previously in RP process network calculations. For some of the nuclei, temperature dependant half-lives were used [13] in the past.

Nucleus	T_z	Previous values (ms)	Present work (ms)	Mean value (ms)	Theoretical prediction (ms)
^{54}Co	0	193.28±0.07 [14]	172±23	193.28±0.07	[13]
^{62}Ga	0	116.4±1.5 [15], 115.95±0.30 [16], 116.34±0.35 [17]	114±2	116.10±0.22	116 [3]
^{66}As	0	95.78±0.39 [16], 95.77±0.28 [18]	97±2	95.79±0.22	96 [3]
^{70}Br	0	80.20±0.80 [16], 78.54±0.59 [18]	79±36	79.12±0.47	79 [3]
^{53}Co	−1/2	240±20 [19]	240±9	240±9	[13]
^{55}Ni	−1/2	204±3 [20]	196±5	202±3	189 [3]
^{57}Cu	−1/2	196.3±0.7 [21]	183±17	196.3±0.7	[13]
^{59}Zn	−1/2	182.0±1.8 [22]	173±14	181.9±1.8	210 [3]
^{61}Ga	−1/2	150±30 [23]	148±19	149±16	150 [3]
^{63}Ge	−1/2	95^{+22}_{-20} [23]	150±9	142±8	95 [3]
^{65}As	−1/2	190^{+110}_{-70} [23]	126±16	128±16	190 [3]
^{67}Se	−1/2	107±35 [24], 60^{+17}_{-11} [25]	136±12	133±11*	106 [3]
^{71}Kr	−1/2	97±9 [26], 64^{+8}_{-5} [25], 100±3 [27]	83±48	100±3*	97 [3]
^{54}Ni	−1	106±12 [20]	103±9	104±7	100 [28]
^{56}Cu	−1	95±3 [29]	82±9	94±3	10 [28]
^{58}Zn	−1	86±18 [30]	83±10	84±9	100 [28]
^{60}Ga	−1	70±15 [31]	70±13	70±10	20 [28]
^{62}Ge	−1		129±35		110 [3]
^{64}As	−1		18^{+43}_{-7}		74 [3]
^{66}Se	−1		33±12		648 [3]
^{70}Kr	−1	57±21 [32]			390 [3]
^{57}Zn	−3/2	40±10 [33]	37±5	38±4	[13]
^{61}Ge	−3/2	40±15 [34]	36±21	39±12	40 [3]

contaminants. For ^{58}Cu, the longer half-life (3.2 s) spreads the decay events over a longer time interval and makes it more difficult to extract a statistically significant value with the present method.

The even-even, $N=Z$ nuclei in this region have half-lives ranging from 17 s (^{72}Kr) to 6.1 d (^{56}Ni). For these long half-lives, our correlation technique no longer works and we should obtain flat time distributions as observed in Fig. 3, where all the time distributions are consistent with half-lives much longer than our correlation interval.

B. $T_z=-1/2$: ^{53}Co, ^{55}Ni, ^{57}Cu, ^{59}Zn, ^{61}Ga, ^{63}Ge, ^{65}As, ^{67}Se, and ^{71}Kr

The $T_z=-1/2$ nuclei ^{61}Ga and ^{65}As were identified as key nuclei for the RP process. If they were unbound, this astrophysical process would be significantly slowed down due to the rather long half-lives of ^{60}Zn and ^{64}Ge [6]. A first half-life determination for these nuclei was performed by Winger *et al.* [23] who showed that these nuclei are sufficiently bound to decay by β^+ decay, so that the RP process would pass through them producing heavier nuclei.

Winger *et al.* [23] measured the half-lives of ^{61}Ga and ^{65}As to be $T_{1/2}=(150\pm30)$ ms and $T_{1/2}=190^{+110}_{-70}$ ms, respectively. These values may be compared to our results (see Fig. 4) of (148 ± 19) ms and (126 ± 16) ms. A good agreement is achieved.

In the cases of ^{53}Co, ^{63}Ge, and ^{67}Se, we obtain results which are roughly a factor of two more precise than previous experimental results. Whereas for ^{53}Co, we find a good agreement with the published value [19], the situation for the two other nuclei is more problematic. Our result for ^{63}Ge matches the one of Winger *et al.* [23] only at the 2σ level. The present result for ^{67}Se is in agreement with a measurement from CERN [24], but in disagreement with an earlier GANIL measurement [25]. A similar disagreement is also found in the case of ^{71}Kr with two recent measurements [27,26]. (Due to the large error bar, our present result for this nucleus is in agreement with all other values.) Although no specific explanation for this anomaly was found, the earlier GANIL half-lives for ^{67}Se, ^{71}Kr, and ^{75}Sr are considerably shorter than all other half-life measurements for the same nuclei. We therefore indicate the values obtained in these measurements in Table I, however, we do not include them when determining average value (see Table I).

Finally, for ^{55}Ni, ^{57}Cu, and ^{59}Zn values in agreement with previous measurements have been obtained. The error

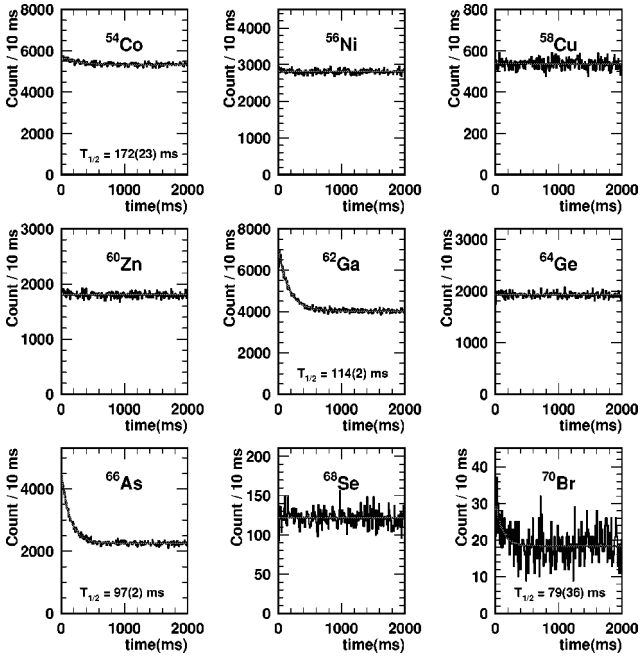

FIG. 3. Decay spectra for the $T_z=0$ nuclei between $Z=27$ and $Z=35$. The decays of ^{62}Ga and ^{66}As are used as reference decays. Although the error bars are larger, the results for the other odd-odd, $N=Z$ nuclei are also in agreement with literature (see Table I). The even-even nuclei show a flat time distribution due to their half-life being much longer than the correlation interval used in the present work.

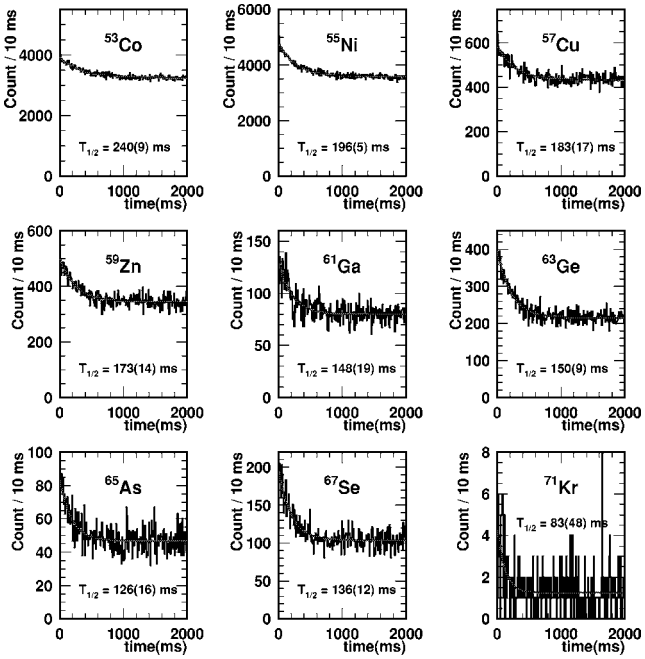

FIG. 4. Decay spectra for the $T_z=-1/2$ nuclei. The half-lives of the RP process key nuclei ^{61}As and ^{65}As as well as for ^{53}Co, ^{63}Ge, and ^{67}Se were measured with improved precision.

bar obtained for ^{55}Ni is comparable with a previous measurement and demonstrates again the reliability of our present data, whereas in the two other cases, the error bars are an order of magnitude larger than previous measurements.

C. $T_z=-1$: ^{54}Ni, ^{56}Cu, ^{58}Zn, ^{60}Ga, ^{62}Ge, ^{64}As, ^{66}Se, and ^{70}Kr

The nuclei ^{60}Ga and ^{64}As may also be important for the RP process. As in the case of ^{61}Ga and ^{65}As, the RP process could pass through these nuclei and proceed to higher masses, if these nuclei are sufficiently bound to decay by β^+ decay. The half-life of these two nuclei as well as the half-life of ^{66}Se observed for the first time by Winger *et al.* [23] and of ^{62}Ge were not known before the present work. Their decay-time distributions are shown in Fig. 5 and the present experimental values are given in Table I. The result for ^{60}Ga of (70 ± 13) ms is consistent with a recent GSI measurement of (70 ± 15) ms from an experiment [31] conducted in parallel with the current work. The result for ^{64}As (18^{+43}_{-7} ms) suffers from very low statistics, resulting in the rather large error bar.

The fit to the data for determining the ^{62}Ge and ^{66}Se half-lives includes the decay of the daughter nuclei ^{62}Ga and ^{66}As, respectively. The time spectrum of the β particles due to the decay chains $^{62}\mathrm{Ge}\rightarrow{}^{62}\mathrm{Ga}\rightarrow{}^{62}\mathrm{Zn}$ and $^{66}\mathrm{Se}\rightarrow{}^{66}\mathrm{As}\rightarrow{}^{66}\mathrm{Ge}$ may be described as follows:

$$N(t)=y_0+N_0\left[1-\frac{\lambda_2 r}{\lambda_1-\lambda_2}\right]\lambda_1 e^{-\lambda_1 t}+N_0\frac{\lambda_1 r}{\lambda_1-\lambda_2}\lambda_2 e^{-\lambda_2 t}, \tag{1}$$

where y_0 is a constant for the background, N_0 is the amount of parent nuclei, λ_1 is the decay constant of the parent, λ_2 is the known decay constant of the daughter, t is the decay time, and r is the ratio of detection efficiencies for the parent and the daughter decay. We assume that the β efficiencies are the same for parent and daughter and set $r=1$. The new half-lives obtained for ^{62}Ge and ^{66}Se are (129 ± 35) ms and (33 ± 12) ms, respectively.

The half-life of ^{54}Ni (Fig. 5) was also determined with the ''parent-daughter'' fit described above, because its decay is followed by the decay of ^{54}Co. A very good agreement was found between the value deduced in the present work of (103 ± 9) ms and the value obtained by Reusen *et al.* [20] of (106 ± 12) ms. This result provides a good test for the daughter decay fit.

The nucleus ^{70}Kr might be of prime interest for the RP process as indicated in the Introduction. The decay of this nucleus was studied for the first time by Oinonen *et al.* [32], where the authors obtained a value of the half-life of (57 ± 21) ms. The decay of ^{70}Kr is followed by the decay of ^{70}Br which has a half-life of (78.54 ± 0.59) ms. Due to poor statistics (see Fig. 5), a fit of the data with the correct curve for a parent-daughter decay was not possible. However, it should be mentioned that, when fixing the ^{70}Kr half-life to the value of Oinonen *et al.* [32], agreement with our experimental data is obtained.

Figure 5 also shows time spectra for the decays of ^{56}Cu and ^{58}Zn with half-life values of (82 ± 9) ms and (83

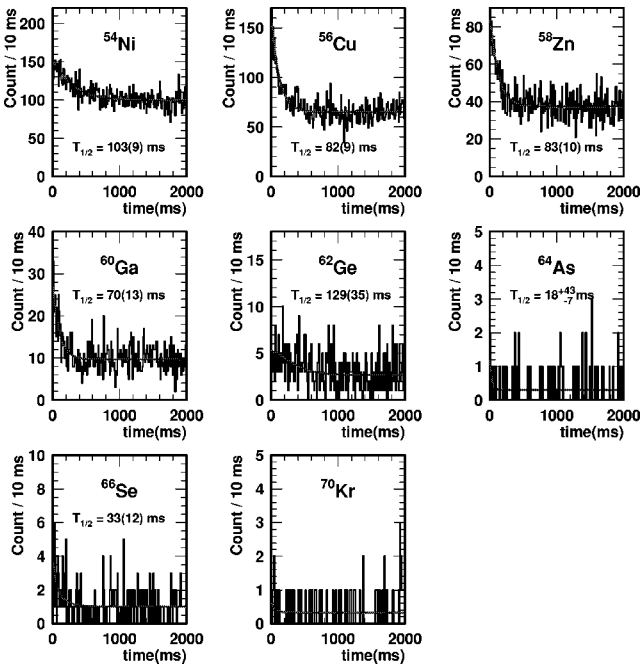

FIG. 5. Decay-time spectra for the $T_z=-1$ nuclei. The half-lives of the four nuclei ^{60}Ga, ^{62}Ge, ^{64}As, and ^{66}Se are determined for the first time in this work (for ^{60}Ga see text). All other results are in agreement with previous measurements (see Table I).

± 10) ms, respectively. These results agree with recent previous work of (95 ± 3) ms [29] and (86 ± 18) ms [30].

D. $T_z=-3/2$: ^{57}Zn and ^{61}Ge

^{57}Zn and ^{61}Ge are the most exotic nuclei produced in this experiment. Both are known β-delayed proton emitters with βp branching ratios of larger than 65% into ^{56}Ni and 80% into ^{60}Zn, respectively. We observe these known decays in our decay-energy spectra. The βp decay is followed by the decay of a short-lived daughter nucleus. Therefore, the half-lives of these nuclei can be determined in two different ways: (i) by fitting the β and βp time spectra with the parent-daughter relation given above, but taking into account the different detection efficiencies for parent and daughter decays and (ii) by gating on events with decay energies larger than 600 keV only involving decays of the parent nucleus (since the daughter does not emit delayed protons). In order to perform the first fit, we have to determine the efficiency ratio r as follows:

$$r=\frac{(1-P_p)\epsilon_\beta}{P_p\epsilon_p+(1-P_p)\epsilon_\beta}, \tag{2}$$

where P_p is the branching ratio of the βp transitions, ϵ_p is the proton efficiency of 100%, and ϵ_β is the β efficiency which we determined to be about 12% by integrating the number of counts under the exponential decay curve and the number of implanted nuclei for several isotopes. Then, the respective values of r for ^{57}Zn and ^{61}Ge are 0.06 and 0.03. Using these values, we obtained a half-life of (36 ± 5) ms for ^{57}Zn which is in agreement with the published value of

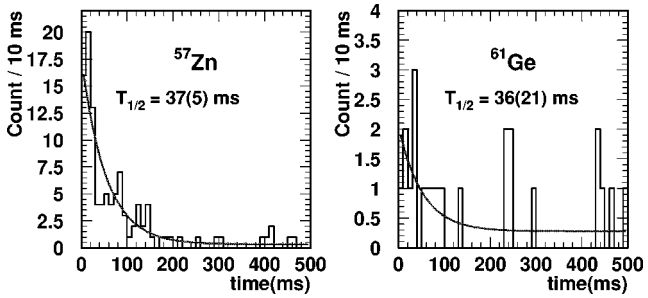

FIG. 6. Decay spectra for the $T_z=-3/2$ nuclei ^{57}Zn and ^{61}Ge. The decay times are generated with a condition on events with decay energies above 0.6 MeV involving only βp events (see text).

(40 ± 10) ms [33]. For ^{61}Ge, however, no fit was possible due to the combined effects of poor statistics and high background.

On the other hand, essentially background-free time spectra can be generated for these two nuclei with a condition on the decay energy selecting events with an energy above 0.6 MeV. In this case, the half-life can be determined by a single-component fit. We obtained a value of (36 ± 21) ms for ^{61}Ge in agreement with a previous measurement yielding (40 ± 15) ms [34]. For ^{57}Zn, the value obtained was (37 ± 5) ms, which is consistent with the one obtained without energy condition. The decay curves and the half-lives determined with this second procedure are presented in Fig. 6.

Table I summarizes our present results and gives error-weighted mean values for the half-lives of all nuclei with $T_z\leqslant 0$ in the region from $Z=27$ to $Z=36$.

IV. ASTROPHYSICAL IMPLICATIONS

As shown in the preceding section the present results are in excellent agreement with other recent measurements. New values have been determined for ^{62}Ge, ^{64}As, and ^{66}Se. In the following section, we will present the results of a theoretical RP-process analysis to study the impact of the new decay rates on the nucleosynthesis and energy generation in an x-ray burst. For this study we used the one-zone self-consistent x-ray burst model described in the literature [4,8]. Figure 7 shows the temperature evolution of the burst with time. The temperature evolution is closely correlated with the nuclear energy release [4,8]. The thermonuclear runaway causes a rapid temperature increase, $t=312$ s after the beginning of the calculation. The peak conditions at $t=314$ s are determined by the ^{56}Ni(p,γ)-^{57}Cu(γ,p) equilibrium [3]. The subsequent cooling phase is characterized by RP-process burning beyond ^{56}Ni until complete hydrogen depletion in the Sn-Sb-Te cycle at $t\approx 520$ s [4]. The β decays of the isotopes discussed here will affect the nucleosynthesis pattern during the thermonuclear runaway phase of the burst and at peak temperature conditions of the burst. Figure 8 shows the reaction path and the reaction flow during the thermonuclear runaway phase and the onset of the cooling phase of the x-ray burst in the mass range considered here. The nuclei for which the half-life is determined in the present work are marked in dark gray. The figure demonstrates that the experiment has successfully investigated all

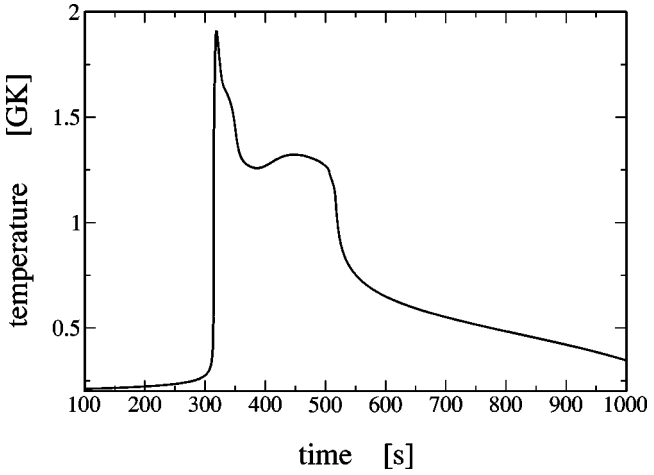

FIG. 7. Temperature evolution during the thermonuclear runaway and the cooling phase of a one-zone x-ray burst model [4,8].

the short-lived β^+ unstable nuclei along the RP-process path in the region between $Z=27$ and $Z=36$.

The most important parameters for studying the impact of nuclear processes in nucleosynthesis scenarios are the associated overall energy release and the evolution of the isotopic abundances. The latter is more sensitive since it is directly associated with the decay or reaction processes in question. Figure 9 shows the evolution of the isotopic abundances of the ^{55,56}Ni and ^{56,57}Cu isotopes during the peak of the burst temperature.

This evolution is determined by the interplay between the β decays, proton-capture reactions, and inverse photodisintegration processes at rapidly changing temperature conditions. At peak temperatures most of the (p,γ) and (γ,p) reactions are in equilibrium and the β^+-decay lifetimes define the time scales of nucleosynthesis evolution.

While most of the previous experimental lifetimes had already been implemented in the reaction rate libraries for RP-process studies before [4], the more recent experimental

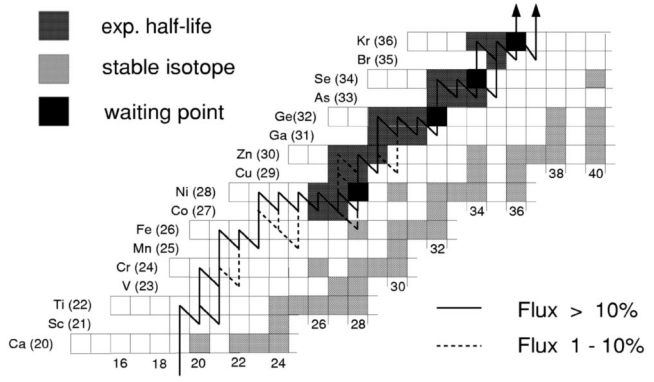

FIG. 8. Results of a RP process network calculation showing the mass flow in the $Z=20$ to $Z=36$ region during the peak temperature phase of the x-ray burst. Stable nuclei are marked in light gray. The nuclei marked in black are the main waiting points along the RP-process path in this mass range. The present experiment has determined the lifetimes of the isotopes marked in dark gray.

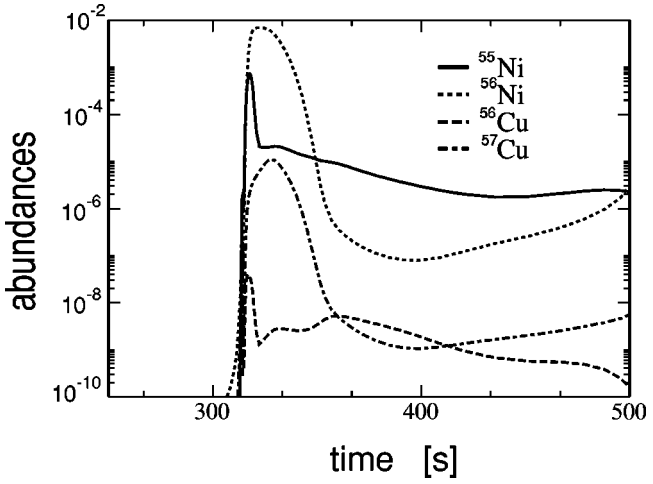

FIG. 9. Abundance evolution of ^{55,56}Ni and ^{56,57}Cu isotopes during the peak temperature conditions of the x-ray burst shown in Fig. 7.

lifetimes for ^{56}Cu, ^{57}Cu, ^{54}Ni, ^{58}Zn, and ^{60}Ga had not yet been included. To study the impact of the experimental results on the RP process, we have compared the RP-process predictions based on these new experimental data with those based on the half-life predictions used for the past RP-process reaction flow simulations [3]. Many of the decay rates of nuclei with $Z\leqslant 30$ are based on the predictions by Fuller, Fowler, and Newman [13] which in addition take into account possible temperature dependent effects. The values for ^{56}Cu, ^{54}Ni, ^{58}Zn, and ^{60}Ga have been based on gross theory predictions [28]. The values for ^{66}Se and ^{70}Kr are based on more recent shell model calculations [3]. Except for the cases of ^{56}Cu, ^{64}As, ^{60}Ga, ^{66}Se, and ^{70}Kr the theoretical predictions are in reasonable agreement with the present experimental values. Therefore, no appreciable difference is expected in the RP-process abundance and time scale simulations for most of the nuclei studied here.

The case is different where substantial discrepancies exist between the predicted and the observed half-lives. In the case of ^{70}Kr a detailed discussion about the reaction flow implications of the experimental results has been given in the paper by Oinonen *et al.* [32]. Similar results have been observed here. In the present discussion we will therefore focus on the implications of the new half-life measurements in the mass 56 to 65 range. The experimental half-life of ^{66}Se is considerably shorter than predicted. However, no consequences for reaction flow or nucleosynthesis could be observed since the time scale and the abundance evolution in this mass range is dominated by the long half-lives of ^{64}Ge and ^{68}Se towards β decay and two-proton capture. Also in the case of ^{60}Ga, no distinct feature could be observed which is explained by the fact that ^{60}Ga is not produced in appreciable amounts by the ^{59}Zn(p,γ) reaction because of the predicted low proton binding energy of ^{60}Ga. The reaction path therefore bypasses ^{60}Ga through the β^+ decay of ^{59}Zn to ^{59}Cu with an experimental half-life in good agreement with the predicted value.

Changes, however, can be observed in the abundance evolution of ^{56}Cu, ^{57}Cu, and ^{55}Ni, ^{56}Ni (see Fig. 10). Devia-

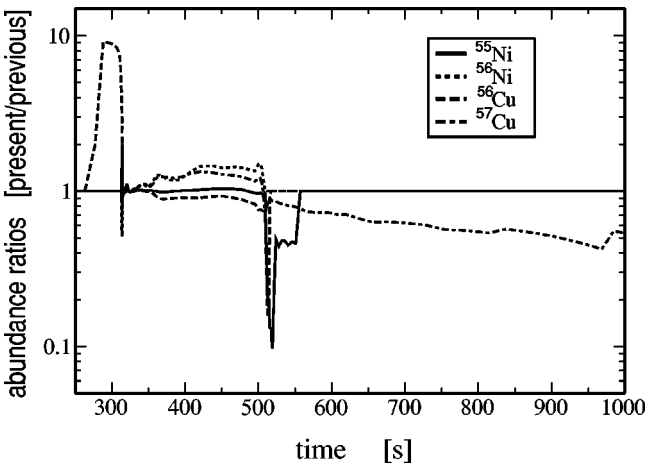

FIG. 10. The figure shows the ratios of the isotopic abundance predictions for ^{55}Ni, ^{56}Ni, ^{56}Cu, and ^{57}Cu derived on the bases of the present β-decay rates and the previous rates shown in Table I as a function of time.

tions in the ^{56}Cu abundance show up in particular in the very early phase of the burst, but more importantly within the first second of the runaway phase ($t=312$ s). During that short time period the higher production of ^{56}Cu is in principle correlated with a lower production in ^{56}Ni. This, however, is not reflected in the figure since the bulk of ^{56}Ni produced at that time results form prerunaway proton capture on ^{54}Fe in the accreted material. During the subsequent cooling phase some deviations can be observed but it becomes again more significant after the depletion of hydrogen towards the end of the cooling phase.

The increase in ^{56}Cu abundance during the early moments of the runaway is due to the fact that at $T<0.5$ GK the ^{56}Cu$(p,\gamma)^{57}$Zn reaction has not reached the ^{56}Cu(p,γ)-^{57}Zn(γ,p) equilibrium. Because of the high Coulomb barrier for proton capture, the β^+-decay of ^{56}Cu is much faster. Since the new experimental ^{56}Cu$(\beta^+\nu)$ rate is significantly slower than the previously used gross theory prediction, the use of the new decay rate causes enrichment in ^{56}Cu and a lower abundance of ^{56}Ni until the ^{56}Ni(p,γ)-^{57}Cu(γ,p) equilibrium is reached which balances the abundances. The deviations in ^{55}Ni and ^{56}Cu abundances at the time of rapid hydrogen depletion is due to the fact that the equilibrium abundances β decay towards the drip line. The deviations are due to the difference in the β-decay rates but have no impact on the temperature and energy generation in the final phase of the x-ray burst.

The experiments have reduced the previous uncertainties and improved the reliability of β-decay rates along the RP-process path. The comparison between simulations based on the previously adopted rates and the new experimental rates shows only miniscule consequences for the nucleosynthesis predictions and no major impact on the overall temperature and luminosity evolution of an x-ray burst. The reduction in uncertainty, however, puts these model predictions on considerably firmer grounds.

V. CONCLUSION

We have determined the half-lives of 22 nuclei produced by projectile fragmentation of a ^{78}Kr beam at 73 MeV/nucleon using the LISE3 separator at GANIL. The half-lives of ^{62}Ge, ^{64}As, and ^{66}Se are obtained for the first time. For almost all other nuclei, a very good agreement was found between previous work and the present data. For most of them, the precision could be improved. The half-life values of all the nuclei are now precise enough in order not to affect the RP process network calculations in a major way.

Nonetheless, higher-precision values might be obtained by increasing the rather low β detection efficiency. Using thicker (1 mm to 1.5 mm) high-quality silicon strip detectors which are now available, efficiencies close to 100% may be reached. In addition, it seems that at these intermediate energies the production of proton-rich nuclei is enhanced when using a fragmentation target of nickel favoring thus proton-transfer reactions from the target nuclei to the projectiles. In fact, despite the higher primary-beam intensity (about a factor of 2), the production rate for proton-rich fragments was much lower (about a factor of 5) than in our previous experiment [7].

ACKNOWLEDGMENTS

We would like to acknowledge the continous effort of the GANIL accelerator staff to provide us with a stable, high-intensity beam. We express our sincere gratitude to the LISE staff for ensuring a smooth running of the LISE3 separator. This work was supported in part by the Conseil Régional d'Aquitaine and the European Community under the Access to Research Infrastructure action of the Improving Human Potential program. P.H.R. ackowledges support from EPSRC (UK).

[1] W. Lewin, J. van Paradijs, and R. Taam, Space Sci. Rev. **62**, 223 (1993).
[2] R.K. Wallace and S.E. Woosley, Astrophys. J., Suppl. **45**, 389 (1981).
[3] H. Schatz *et al.*, Phys. Rep. **294**, 167 (1998).
[4] H. Schatz *et al.*, Phys. Rev. Lett. **86**, 3471 (2001).
[5] S. Goriely *et al.*, Astron. Astyrophys. (submitted); http://arXiv.org/PS_cache/astro-ph/pdf/0201/0201199.pdf
[6] S. Woosley, in Proceedings of the Accelerated Radioactive Beams Workshop, Parksville, Canada, 1985, edited by L. Buchmann and J. d'Auria, p. 4
[7] B. Blank *et al.*, Phys. Rev. Lett. **74**, 4611 (1995).
[8] M. Wiescher and H. Schatz, Prog. Theor. Phys. **140**, 11 (2000).
[9] A.C. Mueller and R. Anne, Nucl. Instrum. Methods Phys. Res. B **56/57**, 559 (1991).
[10] A. Joubert, *et al.*, in *Proceedings of the Second Conference of the IEEE Particle Accelerator, San Francisco, 1991*, edited by L. Lizama and J. Chew (IEEE, Piscataway, NJ, 1991), p. 594.
[11] K. Rykaczewski *et al.*, Phys. Rev. C **52**, R2210 (1995).
[12] C. Longour *et al.*, Phys. Rev. Lett. **81**, 3337 (1998); J. Garcés

Narro *et al.*, Phys. Rev. C **63**, 044307 (2001).
[13] G. Fuller, W. Fowler, and M. Newman, Astrophys. J. **252**, 715 (1982).
[14] V.T. Koslowsky *et al.*, Nucl. Instrum. Methods Phys. Res. A **401**, 289 (1997).
[15] R. Chiba *et al.*, Phys. Rev. C **17**, 2219 (1978).
[16] D.E. Alburger, Phys. Rev. C **18**, 1875 (1978).
[17] C.N. Davids *et al.*, Phys. Rev. C **19**, 1463 (1979).
[18] R.H. Burch, Jr., *et al.*, Phys. Rev. C **38**, 1365 (1988).
[19] J. Honkanen *et al.*, Nucl. Phys. **A496**, 462 (1989).
[20] I. Reusen *et al.*, Phys. Rev. C **59**, 2416 (1999).
[21] D.R. Semon *et al.*, Phys. Rev. C **53**, 96 (1996).
[22] Y. Arai *et al.*, Nucl. Phys. **A420**, 193 (1984).
[23] J.A. Winger *et al.*, Phys. Rev. C **48**, 3097 (1993).
[24] P. Baumann *et al.*, Phys. Rev. C **50**, 1180 (1994).
[25] B. Blank *et al.*, Phys. Lett. B **364**, 8 (1995).
[26] G.T. Ewan *et al.*, Nucl. Phys. **A352**, 13 (1981).
[27] M. Oinonen *et al.*, Phys. Rev. C **56**, 745 (1997).
[28] K. Takahashi, M. Yamada, and T. Kondoh, At. Data Nucl. Data Tables **12**, 101 (1973).
[29] R. Borcea *et al.*, Nucl. Phys. **A695**, 69 (2001).
[30] A. Jokinen *et al.*, Eur. Phys. J. A **3**, 271 (1998).
[31] E. Roeckl *et al.*, Proceedings of the ISOL '01 Conference, Oak Ridge, CA, 2001.
[32] M. Oinonen *et al.*, Phys. Rev. C **61**, 035801 (2000).
[33] A. Jokinen *et al.*, GSI **99-1**, 18 (1999).
[34] M.A.C. Hotchkis *et al.*, Phys. Rev. C **35**, 315 (1987).
[35] J.C. Hardy *et al.*, Nucl. Phys. **A509**, 429 (1990).